



## Research Article

# Development and Characterization of an *Ex Vivo* Arterial Long-Term Proliferation Model for Restenosis Research

Daniela Haase<sup>1</sup>, Sylvia Otto<sup>1</sup>, Bernd F. M. Romeike<sup>2</sup>, Hans R. Figulla<sup>1</sup> and Tudor C. Poerner<sup>1</sup>

<sup>1</sup>Clinic of Internal Medicine I, Jena University Hospital, Friedrich Schiller University of Jena, Germany; <sup>2</sup>Institute of Pathology, Jena University Hospital, Friedrich Schiller University of Jena, Germany

### Summary

One of the main limitations of percutaneous coronary interventions is restenosis, occurring in small-diameter arteries. Many efforts are underway to find improved intracoronary devices to prevent in-stent restenosis. The aim of this study was to produce a new *in vitro* test platform for restenosis research, suitable for long-term cell proliferation and migration studies in stented vessels. Fresh segments of porcine coronary arteries were obtained for decellularization and were then reseeded with human coronary artery endothelial (HCAEC) and human coronary artery smooth muscle cells (HCASMC). Subsequently, bare metal stents (BMS) or drug eluting stents (DES) were implanted and the segments were reseeded with HCAEC and HCASMC for up to three months. The stented segments were examined at time zero and after 2, 4, 6, 8 and 12 weeks by histochemical and immunohistochemical characterization and the reseeded areas before and after stent implantation were measured. Cells formed multiple layers after three months and detection of both CD31 and  $\alpha$ -smooth muscle actin by specific antibodies showed that HCAEC and HCASMC are adherent and growing in several layers. Furthermore, we could show a significantly smaller proliferation area in DES ( $70\% \pm 3.5\%$ ) compared to BMS ( $17\% \pm 2.3\%$ ). These data are similar to animal and human studies. Therefore, this vessel model might be suitable as an initial benchmark for testing new anti-proliferative endovascular therapies and could consequently help to reduce animal experiments in this research area.

Keywords: restenosis, coronary arteries, decellularization, reseeded

## 1 Introduction

Cardiovascular disease is the leading cause of mortality in Europe and the United States (Lloyd-Jones et al., 2009). Endovascular stents have lowered acute complication rates and improved long-term follow-up of coronary interventions, which are mainly limited by the occurrence of restenosis (Gruberg et al., 2000).

Restenosis is basically due to neointimal hyperplasia triggered by lesions of the vessel wall during stent implantation (Rosanio et al., 1999). Endothelial cells of the intima as well as inflammatory cells from subintimal layers release cytokines that induce vascular smooth muscle cells (SMC) to migrate from the media to the intima and proliferate (Salabei and Hill, 2014). Therefore, drug eluting stents (DES) have been developed, which slowly release

anti-proliferative substances to the surrounding tissue (Katz et al., 2015). Despite a reduction of the restenosis rate in DES compared with bare metal stents (BMS), late in-stent restenosis (ISR) has not been abolished (Stefanini and Holmes, 2013; Stettler et al., 2007; Akin et al., 2011). The mechanisms leading to DES restenosis are the development of neoatherosclerosis and also local inflammatory processes triggered by the anti-proliferative substance, the polymer, or the stent struts themselves (Byrne et al., 2009; Pfisterer et al., 2006). Currently available DES elute mainly mTor inhibitors (sirolimus, everolimus, biolimus or zotarolimus) and less paclitaxel, with or without a polymeric carrier (Sanchez et al., 2015; Sheth and Giugliano, 2014). The anti-proliferative effects are obtained at the cost of a significantly prolonged period of endothelialization of the stent struts and thus a dual anti platelet therapy (DAPT) of at least 6 months is indicated for DES

Received March 5, 2015;  
Accepted September 10, 2015;  
Epub September 24, 2015;  
<http://dx.doi.org/10.14573/altex.1503051>



This is an Open Access article distributed under the terms of the Creative Commons Attribution 4.0 International license (<http://creativecommons.org/licenses/by/4.0/>), which permits unrestricted use, distribution and reproduction in any medium, provided the original work is appropriately cited.

**Tab. 1: Methods of decellularization**

	Chemical	Enzymatic	Physical
<b>A</b>	4% sodium deoxycholate (90 min)	DNase I (2 h)	agitation (RT)
<b>B</b>	0.5% sodium dodecyl sulfate 0.5% sodium deoxycholate (3x12 h)	–	agitation (RT)
<b>C</b>	0.25% polyethylene glycol 0.5% sodium dodecyl sulfate (3x12 h)	DNase I (2 h)	agitation (RT)
<b>D</b>	4% sodium deoxycholate 0.25% Triton X-100 (24 h)	DNase I RNase A (24 h)	agitation (37°C)

RT = room temperature

whereas a 4-week DAPT is regarded sufficient after BMS implantation for prevention of stent thrombosis (Kolh et al., 2014). Therefore, many efforts are underway to find the ideal trade-off between selective inhibition of the proliferation and migration of smooth muscle cells on one side and delayed stent coverage on the other (Nakazawa et al., 2008, 2011).

The goal of the present study was to produce an *in vitro* vessel model for DES testing, which should spare animal experiments by eliminating devices that have either insufficient anti-proliferative properties or induce cytotoxic reactions in endothelial cells.

## 2 Materials and methods

### 2.1 Specimen

All animal samples were obtained from waste of the local slaughterhouse. Freshly excised segments of porcine coronary arteries (4 mm diameter, 6–10 cm length) were separated from surrounding tissue prior to decellularization. Each vessel was divided into one control sample and one sample undergoing the decellularization procedure. For mechanical testing, the segments had a length of at least 8 cm.

### 2.2 Decellularization

For decellularization, several protocols were tested. The combinations of chemical, enzymatic and physical treatment are shown in Table 1. For all protocols, each incubation step was followed by a 24 h washing step with PBSA (phosphate buffered saline including 1% penicillin/streptavidin and 1% partricin A, PAA, Linz, Austria).

All treated and untreated samples were subsequently stored in sterile PBSA at 4°C.

### 2.3 Verification of decellularization

#### *Histological staining and microscopy*

Histological examination of samples underlying decellularization and of control samples was performed using hematoxylin-eosin (HE), Elastica-van-Gieson (EvG) and 4',6-diamidin-2-phenylindol (DAPI) staining.

For HE staining, paraffin-embedded tissue was cut into 5  $\mu$ m sections using a rotary microtome (RM 2165, Leica, Wetzlar, Germany), transferred to slides and dewaxed, followed by 5 min incubation in Mayer's hematoxylin (Roth, Karlsruhe,

Germany), 5 min wash in running tap water and 3 min incubation in eosin solution (0.5%, Roth). EvG staining was done by 1 h incubation in Weigert's resorcin-fuchsin solution (Roth), iron hematoxylin (Roth) for 3 min and van-Gieson-solution (Hollborn, Leipzig, Germany) for 10 min. For DAPI staining, paraffin-embedded samples were mounted with Vectashield Mounting Medium for fluorescence (Vector Laboratories, Inc., CA, USA). After staining, slides were imaged by light and fluorescence microscopy (AxioVision, Zeiss, Jena, Germany) using 100 x, 200 x and 400 x objectives.

#### *DNA analysis*

Genomic DNA of decellularized and non-decellularized arterial tissue was isolated using the DNeasy tissue kit (Qiagen, Hildesheim, Germany) according to the manufacturer's instructions. The presence or absence of genomic DNA was proven by spectrophotometric measurement at 260/280 nm (NanoDrop Technologies Inc., Wilmington, USA) and agarose gel electrophoresis.

#### *Mechanical characterization*

The mechanical behavior of the decellularized versus non-decellularized tissue was assessed using a stretch test and an opening angle test.

For the stretch test, arterial segments of equal length and thickness were clamped in a TIRAtest 2420 machine (TIRA GmbH, Schalkau, Germany) and expanded under uniaxial loading at a rate of 10 mm/min as previously described (Bolland et al., 2007). Pull-out forces at elongations of 20 and 30 mm were recorded in Newton (N) and calculations were performed using the TIRAsoft software (TIRA GmbH, Schalkau, Germany).

Fresh arterial and decellularized arterial segments were cut into ring segments ( $n = 5$  per sample) to prepare the opening angle test as previously described (Williams et al., 2009). Rings were equilibrated in isotonic saline solution for 30 min, radially cut and again equilibrated for 30 min. Images were taken using a digital camera and the opening angle was measured using ImageJ 1.4.3 software (National Institutes of Health, USA).

These experiments were repeated three times.

### 2.4 Cell culture and scaffold seeding

The primary cell lines HCASMC (human coronary artery smooth muscle cells) and HCAEC (human coronary artery

endothelial cells) were purchased from Lonza (Basel, Switzerland). Cells were maintained in Smooth Muscle Cell Growth Medium 2 and Endothelial Cell Growth Medium, respectively (PromoCell, Heidelberg, Germany) at 37°C in 5% CO<sub>2</sub>. For reseeding of scaffolds, 1x10<sup>4</sup> cells per cm<sup>2</sup> were added three times a week. Cells were pipetted directly into the lumen of the vessel; allowed to settle for 15 min and then the vessel was axially rotated by 90 degrees. This procedure was repeated three times until the entire lumen was seeded, and then medium was added back. Parallel samples were run for HCASMC and HCAEC, respectively, and for HCASMC and HCAEC in culture.

## 2.5 Stent implantation

To investigate the effects of coronary stents on the reseeded vessels, we implanted different DES (4 paclitaxel [TAXUS<sup>®</sup> Express2<sup>™</sup>, Boston Scientific], 4 everolimus [XIENCE V<sup>®</sup>, Abbott Vascular] and 2 zotarolimus [Resolute<sup>®</sup> Integrity, Medtronic] eluting stents) and 2 different bare metal stents (DRIVER<sup>®</sup> Sprint, Medtronic and MULTI-LINK ZETA<sup>®</sup>, Abbott Vascular). The stented vessels were seeded with HCASMC and HCAEC and samples were collected at time zero and after 2, 4, 6, 8 and 12 weeks.

## 2.6 Cell growth assays

To test for cytotoxic components remaining after the decellularization procedure, cell seeding experiments were performed under standard culture conditions. A 1 cm<sup>2</sup> sheet of decellularized specimen was put into the well of a 24-well culture plate. The assay was performed as previously described (Kimuli et al., 2004). Briefly, smooth muscle cells and endothelial cells (passage 4, at a density of 1 x 10<sup>4</sup> cells/10 μl) were added to the luminal surface of the specimen. Cells were cultured in appropriate growth medium. After an incubation period of 1 or 14 days, specimens were washed three times with PBS and incubated with 10 μM calcein-AM (Life Technologies Inc., Darmstadt, Germany) for 30 min at room temperature. Images were acquired using an inverse microscope (Axiovert, Zeiss, Jena, Germany).

Cell viability assays were performed as previously reported (Haase et al., 2010). Briefly, cells were seeded in the lumen of stented and non-stented decellularized scaffolds. After 0 h and after 2, 4, 6, 8 and 12 weeks, a sample of 1 cm length was cropped, radially cut and 10 μl of 5 mg/ml (3-(4,5-dimethylthiazol-2-yl)-2,5-diphenyltetrazolium bromide (MTT, Sigma-Aldrich, Taufkirchen, Germany) was added for 4 h. Then 100 μl of solution buffer (10% SDS, 0.01 M HCl) was added for overnight incubation. Samples were transferred to a 96-well plate and absorbance at 570 nm was measured. These experiments were carried out in replicates of five.

## 2.7 PCR

Total RNA from arterial vessels reseeded for 12 weeks was extracted with the RNeasy Mini Kit (QIAGEN, Hilden, Germany) according to the manufacturer's instructions. RNA was adjusted to 1 μg/10 μl for reverse transcription (Reverse Transcription System, Promega, WI, USA). CD31, alpha-

smooth muscle actin (α-SMA) and beta-actin expression levels were analyzed by PCR on the UNO II cycler (Biometra, Göttingen, Germany) using the DyNAzyme DNA Polymerase Kit (Finnzymes, MA, USA). The sequences of the primers were as follows: CD31(sense) 5'-ATGGGTGCAGTTCCA TTTTC-3'; CD31(antisense) 5'-CAGGTGTGCGAAATGC TCT-3'; α-SMA(sense) 5'-CCATCACAATGCCTGTGGTA -3'; α-SMA(antisense) 5'-GATGACCCAGATCATGTT TGA-3'; beta-actin(sense) 5'-ACCACCCCAGCCATGTACG-3'; beta-actin(antisense) 5'-ATGTCACGCACGA-TTTCCC-3'. Cycling conditions were as follows: 10 min initializing denaturation, followed by 40 cycles of 95°C for 20 s, 55°C for 20 s (58°C for CD31 and α-SMA) and 72°C for 30 s. PCR products were analyzed by agarose gel electrophoresis.

## 2.8 Free float staining and embedding of stented scaffolds

The stented scaffolds were stained in the appropriate solutions in 15 ml tubes. Steps for HE and EvG staining were approached as described above. After staining, specimens were dehydrated, dried and embedded in a synthetic resin (Spezifix 20, Struers, Ballerup, Denmark). Sawing was performed using a low speed precision saw (ISOMET, Buehler, Illinois, USA) and the resulting sections were ground to 300 μm thickness using the grinder PHOENIX 400 (Buehler, Illinois, USA) and abrasive paper.

## 2.9 Immunostaining

Immunostainings of CD31 and alpha-smooth muscle actin in fresh tissue sections were performed using polyclonal CD31 (Dako, Hamburg, Germany) and alpha-smooth muscle actin (Abcam, Cambridge, UK) antibodies at a concentration of 1:500 for 1 h at room temperature, followed by Cy-3 and Cy-2-conjugated secondary antibody (Beckman, CA, USA) incubation for an additional 1 h in the dark. Nuclei were stained using mounting medium containing DAPI (Vector Laboratories, Inc., CA, USA). Images were taken with a laser scanning microscope (LSM510, Zeiss, Jena, Germany).

## 2.10 Data analysis and statistics

For analysis of cell growth inhibition after stent implantation, images were taken before and after stent implantation using a light microscope (Axioplan 2, Zeiss, Jena, Germany). The reseeded area was defined as the area between the outside of the vessel and the vessel lumen and was measured using ImageJ software (version 1.4.3, National Institutes of Health, USA). After 12 weeks of reseeding (day of stent implantation [t0]), the measured area of a vessel was defined as 100% and all following measurements of the same vessel were related to this.

Statistical analysis was performed using SPSS for Windows (version 13.0). Continuous variables are given as mean values ± SD. Stretch test, opening angle test and cell growth inhibition were analyzed for statistically significant differences by Student's two-tailed t-test for unpaired samples. Differences with p ≥ 0.05 are defined as not significant. Significant p-values are indicated with asterisks.



### 3 Results

#### 3.1 Characterization of decellularized arterial vessels

Compared to native vessels, a complete decellularization was obtained with protocol D (see Tab. 1; Fig. 1A). This was confirmed by the complete absence of DNA fragments. EvG staining and microscopic evaluation demonstrated hardly any differences between control segments and completely decellularized segments regarding the structure of the extracellular matrix (Fig. 1B-D). The stretch test revealed no significant

differences between fresh and decellularized vessels in the applied force for an elongation of 20 mm ( $8.87 \pm 0.57$  N and  $10.03 \pm 1.83$  N;  $p = 0.414$ ) and 30 mm ( $18.47 \pm 2.26$  N and  $21.31 \pm 1.56$  N;  $p = 0.147$ ) (Fig. 2A).

Also, native vessels had no significantly greater opening angles compared with the decellularized vessels ( $66.8 \pm 7.4^\circ$  and  $49.1 \pm 9.8^\circ$ ;  $p = 0.0518$ ), indicating no significant reduction in the tensile stresses after decellularization (Fig. 2B).

A monolayer of HCASMC and HCAEC could be detected on the luminal surface of the decellularized specimen 14 days after cell seeding (Fig. 3A). Control wells without the arterial sam-

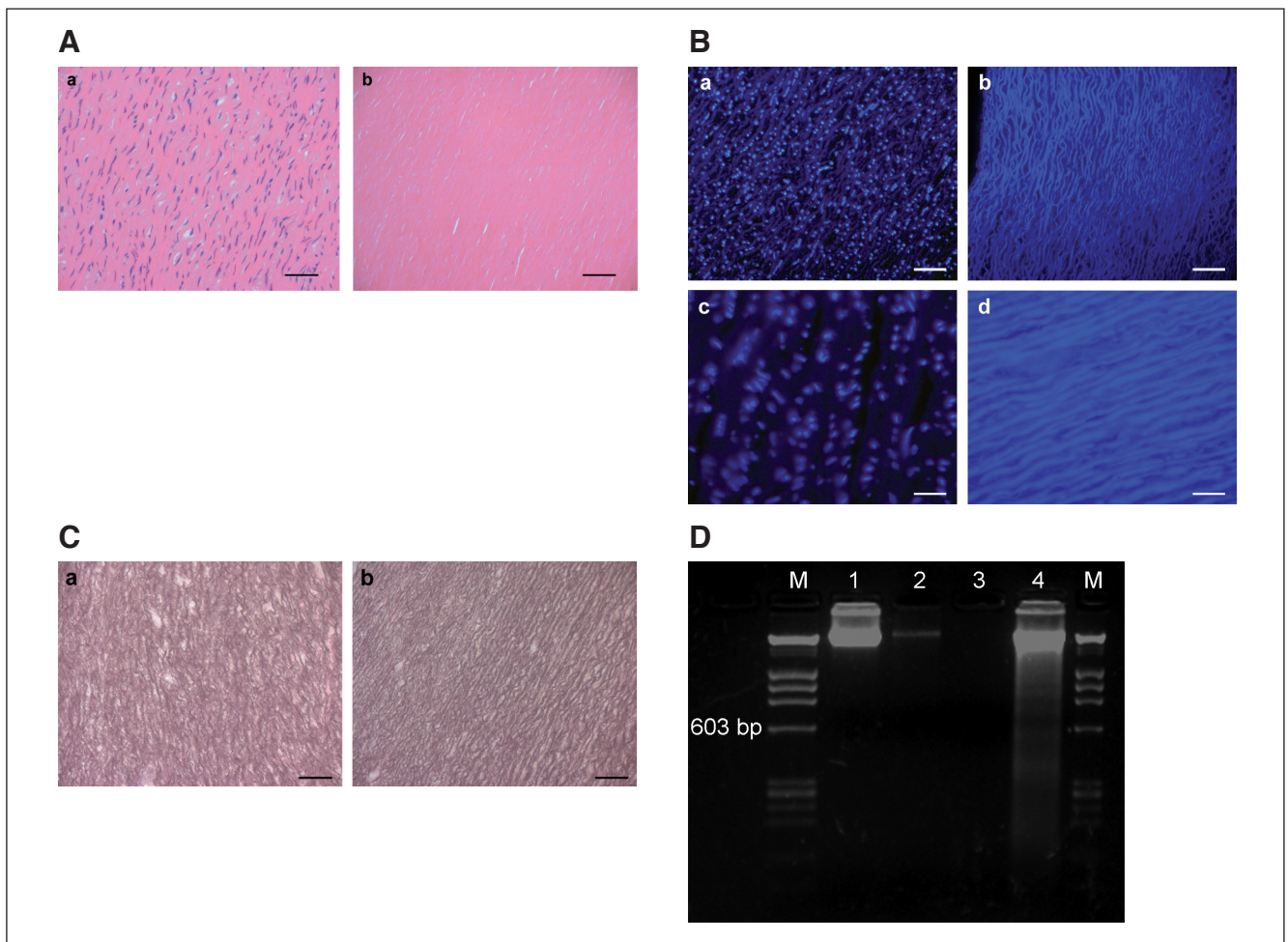


**Fig. 1: Treatment with 4% sodium deoxycholate, 0.25% Triton X-100 and subsequent incubation with DNase I and RNase A results in complete decellularization**

A: Paraffin-embedded sections of porcine artery before and after decellularization. HE staining reveals blue-stained cell nuclei in the control segment (a) and complete decellularization in treated segments (b).

B: DAPI staining before (a, c) and after (b, d) decellularization treatment. The luminous blue color indicates the nuclei. Images (c) and (d) are higher magnifications of (a) and (b), respectively.

C: EvG staining shows the structure of the elastic (black-violet) and collagen (pink-red) fibers without differences between control (a) and completely (b) decellularized segments.

D: Gel electrophoresis confirms the complete absence of DNA fragments using protocol D. Lanes 1, 2 and 4 show residual genomic DNA, whereas lane 3 is completely free of DNA. Legend: (M) standard DNA ladder, (1, 2) partially decellularized artery, (3) completely decellularized artery, according to protocol D, (4) control arterial segment.

Scale bars 100  $\mu$ m; in 1B scale bars 100  $\mu$ m (a, b) and 50  $\mu$ m (c, d).

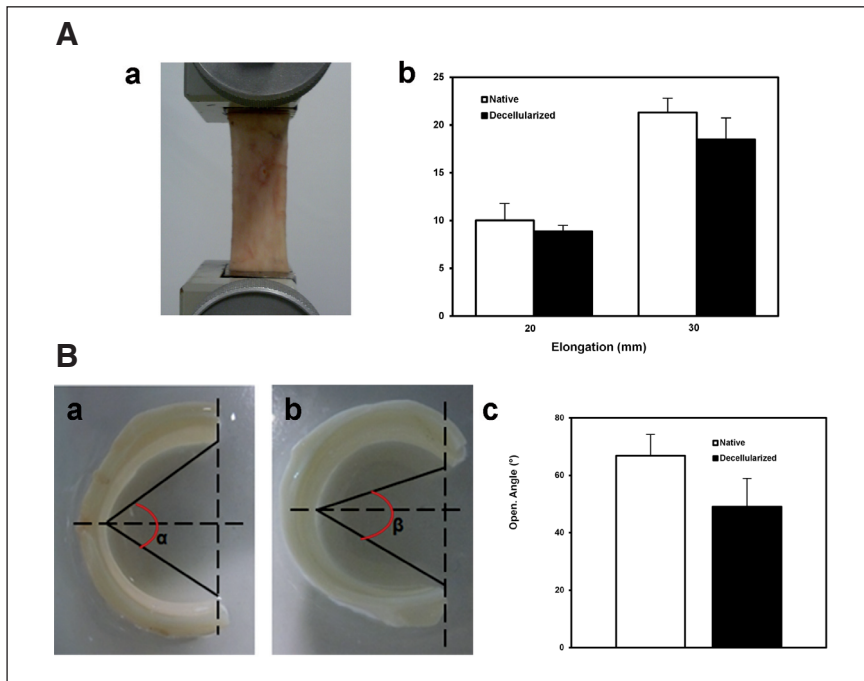


**Fig. 2: Decellularization does not affect mechanical properties of the arterial tissue**

A: (a) Example of an arterial segment subjected to a stretch test using the TIRAtest 2420 machine. (b) Decellularized vs. non decellularized arterial segments underwent mechanical stretching. The graph shows no significant differences between the groups. Segments were expanded under uniaxial loading at a rate of 10 mm/min. Pull-out force (in Newton) was measured after an elongation of 20 and 30 mm (mean values  $\pm$  SD,  $n = 3$ ;  $p \geq 0.05$ ).

B: Representative images for native (a) and decellularized (b) arterial segments for opening angle measurement ( $\alpha = 64^\circ$ ,  $\beta = 48^\circ$ ). (c) Opening angles in native arteries were not significantly greater compared with decellularized ones, indicating no reduction in tensile stresses after decellularization ( $n = 15$ ;  $p \geq 0.05$ ).

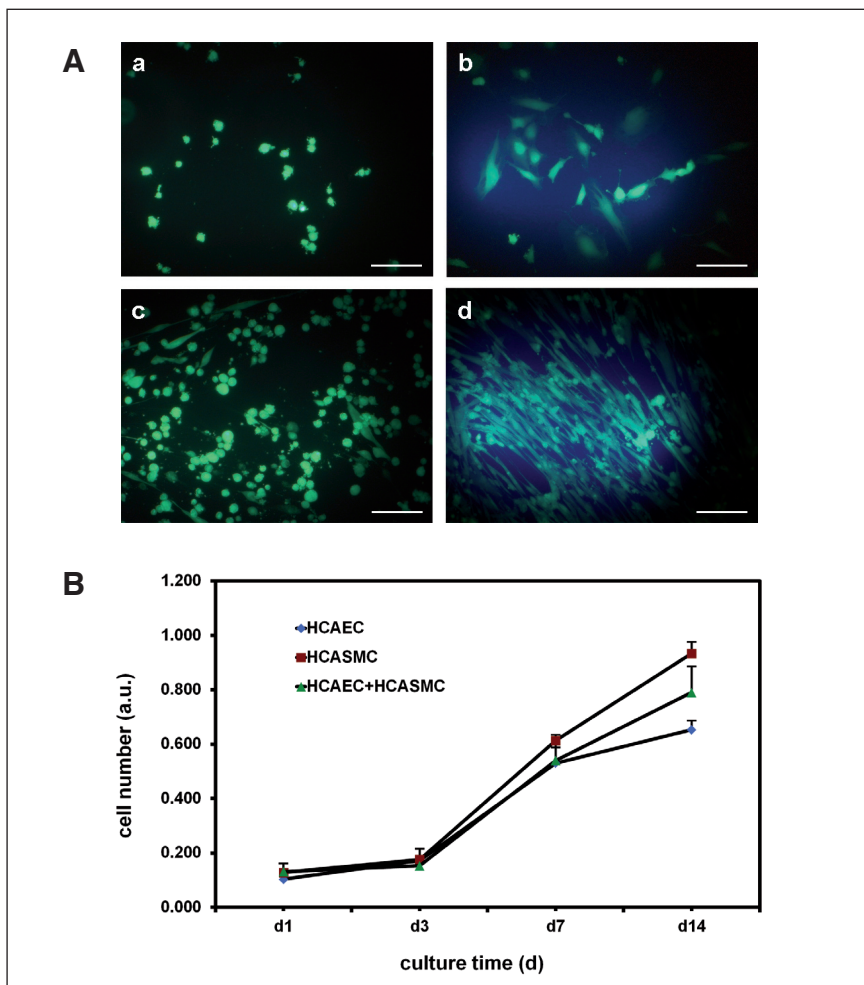


**Fig. 3: Decellularization conditions do not cause cytotoxicity of the matrix**

A: Fluorescence imaging of endothelial (a, b) and smooth muscle cells (c, d) seeded on a decellularized porcine artery and stained with calcein-AM; (a, c) after 1 day of culture, (b, d) after 2 weeks of culture. Scale bars 100  $\mu$ m.

B: MTT assay shows no significant differences in the cell viability of HCAEC, HCASMC and both cell lines in co-culture.



ples also formed a confluent monolayer. The cell viability assay showed that both cell lines alone or in co-culture were able to grow on the decellularized matrix in the same manner as under standard cell culture conditions (Fig. 3B).

### 3.2 Assessment of neointimal proliferation

Fourteen days after reseeding, HCASMC and HCAEC formed a confluent monolayer and after three months multiple layers were observed (Fig. 4A). Adherence of cells did not differ between

the cell lines alone and in co-culture as shown by HE staining. RT-PCR of the reseeded vessels showed distinct bands for HCAEC-specific (CD31) and HCASMC-specific ( $\alpha$ -smooth muscle actin) primers (Fig. 4B). Detection with CD31 and  $\alpha$ -smooth muscle actin specific antibodies showed that both HCAEC and HCASMC are adherent on the decellularized matrix and growing in several layers (Fig. 4C). Thus, optimal cell growth to mimic in-stent proliferation could be achieved by reseeding the decellularized scaffold with both cell lines in co-culture over 12 weeks.

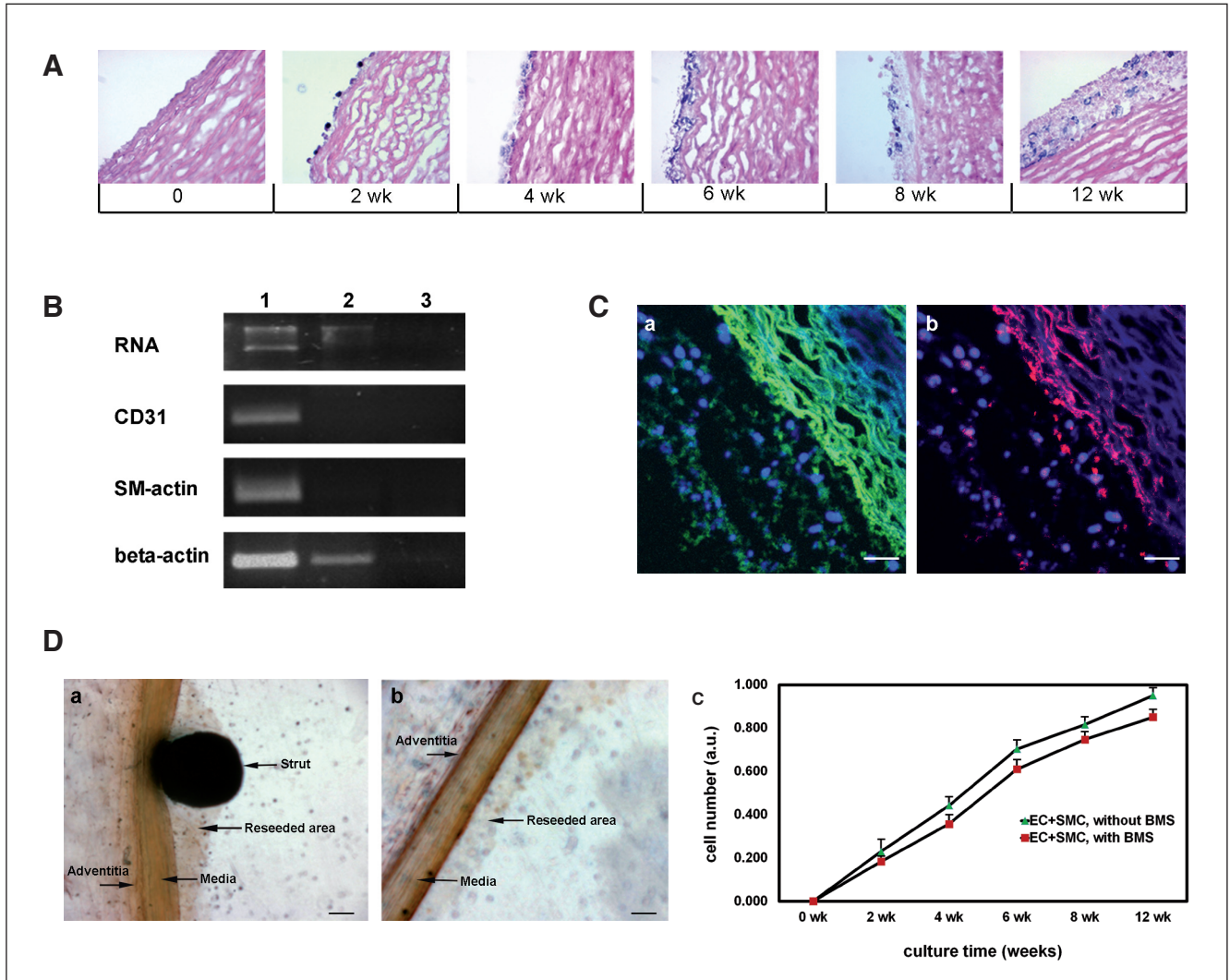


**Fig. 4: Reseeding with human coronary artery endothelial (HCAEC) and human coronary artery smooth muscle cells (HCASMC) mimics neointima proliferation**

A: HE staining of frozen sections of reseeded (HCAEC and HCASMC in co-culture) arterial segments over a time period of 12 weeks, showing multiple cell layers after three months.

B: PCR analysis of porcine artery, reseeded for 12 weeks. RT-PCR was done for  $\beta$ -actin,  $\alpha$ -smooth muscle actin and CD31.

Legend: (1) reseeded artery; (2) before decellularization; (3) after decellularization.

C: Immunofluorescence labelling of reseeded segments with (a) anti human  $\alpha$ -smooth muscle actin (green) and (b) anti human CD31 (red) antibodies. Nuclei are stained with DAPI (blue); images were taken with the LSM510, Zeiss.

D: EvG staining of decellularized arterial segments, reseeded with HCAEC and HCASMC with (a) and without (b) implantation of a bare metal stent. MTT assay shows little difference in the cell viability of stented and non-stented segments over the whole time period (c). Scale bars in C = 50  $\mu$ m; in D = 100  $\mu$ m. a.u. = arbitrary units.

Additionally, cell growth was compared between BMS-stented and non-stented vessel segments. There was no significant difference in the formation of the cell layers over the whole time period of 12 weeks ( $p = 0.138$ , Fig. 4D).

### 3.3 Inhibition of neointimal proliferation

To evaluate anti-proliferative effects on the engineered vessel segments, we implanted DES and BMS in the samples reseeded with HCAEC and HCASMC and examined them by EvG stain-

ing and immunohistochemistry at 2, 4, 6, 8 and 12 weeks compared to baseline. In all stent systems the proliferation area was significantly smaller in the DES compared to BMS ( $p = 0.0007$ ; Fig. 5A-B). A maximum inhibition of cell growth could be observed in the first six weeks in the DES, whereas only a slight cell decrease could be observed in the BMS over the whole time period ( $70 \pm 3.5\%$  and  $17 \pm 2.3\%$ ;  $p = 0.0003$ ). No significant differences between different brands of DES were observed ( $p = 0.074$ ; Tab. 2). Detection with CD31 and  $\alpha$ -smooth mus-

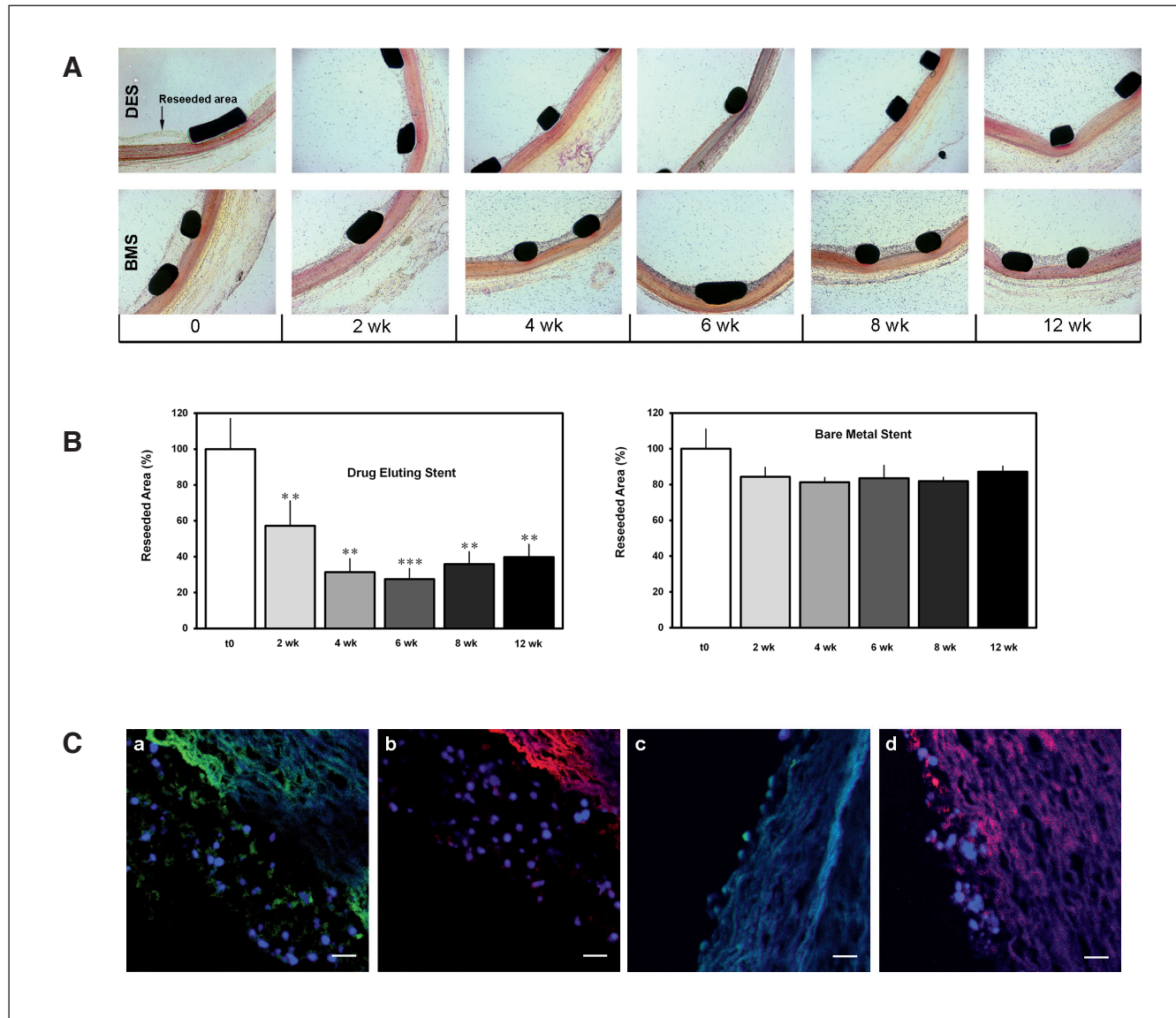


**Fig. 5: Comparison of BMS and DES in reseeded vessels**

A: EvG staining of reseeded arterial vessels after 12 weeks of stent implantation. Comparison of drug eluting stent (DES) versus bare metal stent (BMS).

B: Significant reduction of the proliferation area in DES-stented vessels. Images of six positions were taken 0 h, 2, 4, 6, 8 and 12 weeks after stent implantation, and the area of cell growth was quantified (mean values  $\pm$  SD, p-value: \*  $\leq 0.05$ , \*\*  $\leq 0.01$ , \*\*\*  $\leq 0.001$ ).

C: Immunofluorescence labelling of stented segments after 6 weeks with (a, c) anti human  $\alpha$ -smooth muscle actin (green) and (b, d) anti human CD31 (red) antibodies. Nuclei are stained with DAPI (blue). (a, b) BMS-stented; (c, d) DES-stented segments. Scale bars 50  $\mu$ m.

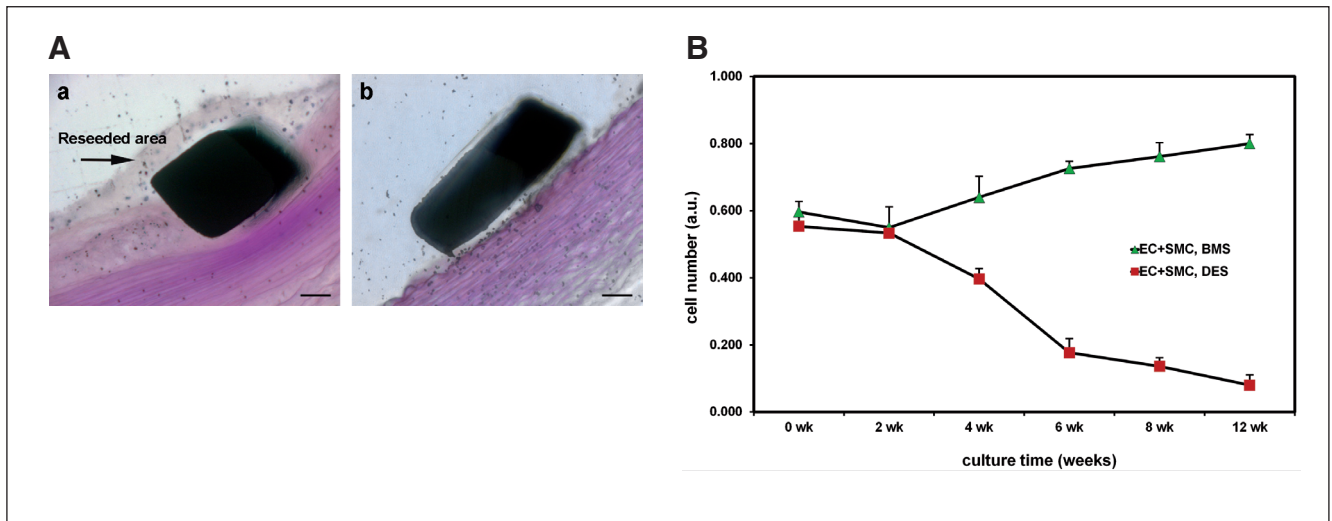


**Fig. 6: Significant cell mass reduction in DES-stented vessels**

A: HE staining of reseeded vessels after 6 weeks of BMS (a) and DES (b) implantation, respectively. Scale bars 100  $\mu$ m.

B: MTT assay confirms significantly reduced cell viability in DES-stented vessels compared with BMS-stented vessels over a time period of 12 weeks. a.u. = arbitrary units.

cle actin specific antibodies revealed that both, HCAEC and HCASMC proliferation was reduced in comparative amounts in the DES (Fig. 5C).

Additionally, the cell decrease was determined by measuring the cell viability of the stented vessels by MTT assay at the same time points (see above). Results indicated a significantly lower number of cells in the DES-stented vessels compared to BMS-stented vessels, with the greatest differences between 6 and 8 weeks ( $p = 0.0002$ ; Fig. 6).

#### 4 Discussion

The aim of our study was to engineer an *in vitro* model able to investigate the anti-proliferative effects of new candidate agents.

Initially, in order to design a scaffold for tissue engineering, we developed a decellularization protocol for arterial vessels. In the past, decellularized blood vessels have been studied for their potential use as vascular grafts for small diameter arteries (Antonova et al., 2008; Borschel et al., 2005; Jo et al., 2007; Schaner et al., 2004; Gui and Niklason, 2014). They consist of a natural extracellular matrix, have very low immunogenicity and can be reseeded with various cells of choice and for any period of time (Teebken et al., 2009; Amiel et al., 2006). Though numerous decellularization protocols exist, there was no satisfying procedure for modeling the *in vivo* situation due to significantly altered mechanical characteristics compared to native vessels (Roy et al., 2005; McFetridge et al., 2004).

In this study, we present a new decellularization protocol for small diameter vessels which preserves the composition and mechanical behavior of the extracellular matrix (ECM) with-

**Tab. 2: Comparison of different brands of DES and BMS**

DES	proliferation area after 6 weeks (%)	proliferation area after 12 weeks (%)
TAXUS® Express2	29 $\pm$ 4.2	48 $\pm$ 7.9
XIENCE V®	28 $\pm$ 7.1	39 $\pm$ 5.5
Resolute® Integrity	33 $\pm$ 6.7	40 $\pm$ 6.3
BMS		
DRIVER® Sprint	81 $\pm$ 10.4	88 $\pm$ 10.9
MULTI-LINK® ZETA	85 $\pm$ 9.1	86 $\pm$ 7.7

out increased stiffness. Despite the existence of various decellularization protocols, e.g., for bladder (Bolland et al., 2007) and heart valves (Rieder et al., 2004; Teebken et al., 2009), the efficiency of a method depends mainly on the tissue type. Previously described protocols (Dahl et al., 2003; Williams et al., 2009) did not work properly for arterial vessels.

Of particular interest was the work of Fitzpatrick et al. (2010), who described the decellularization of a porcine descending aorta by using 0.25% sodium-deoxycholate. Since we could not reproduce this condition for a complete decellularization of the arteries, we changed the incubation time and the composition of the chemicals in different steps and found that a high working concentration (4%) of the ionic detergent sodium-deoxycholate in combination with a low amount of the non-ionic detergent Triton X-100 led to complete decellularization. Additionally, all incubation steps were carried out at 37°C.

According to Gilbert et al. (2006), sodium-deoxycholate is more disruptive than sodium-dodecyl-sulphate (SDS), resulting in a higher damage of the elastic fibers. However, we could not find a degradation of elastic fibers or loss of collagen content as shown by EvG staining. Furthermore, no significant differences in the mechanical behavior of the extracellular matrix could be observed; however, there is a trend towards more stiffness of the decellularized specimen, indicating a minimal alteration of the ECM as a result of the chemical treatment.

Moreover, attention should be paid to the removal of residual chemicals before the further use of such scaffolds. An insufficient removal of the decellularization components may lead to cell damage or in an *in vivo* setting to an immune response by the host (Rieder et al., 2006). To exclude this potential upset, washing conditions were extended over longer time periods and a cell growth assay was performed to assess the potential cytotoxicity of the decellularized matrix. The resulting viability and adherence of the seeded cells indicate that the decellularized scaffold is not cytotoxic and therefore suitable for further reseeding experiments.

To mimic the formation of a neointima inside the vessels, we reseeded the decellularized matrix with EC and SMC. In standard cell growth assays we observed that SMC grew 3 times faster than EC, so the supposed ratio between SMC and EC on the reseeded vessels is 1:3. This was confirmed by the immunohistochemical data. Because the neointima consists mainly of SMC, this ratio seems representative enough to measure distinct anti-proliferative effects on SMC and EC in this *in vitro* model.

The process of clinical restenosis proceeds slowly and continuously within the first months after stent implantation, which is the reason why DES release the drug over a long time period (Dangas et al., 2010). In a next step we investigated the effect of BMS and several DES on the reseeded vessels over a time period of 12 weeks. After stent implantation in our model, the expected significant differences in cellular proliferation rates between DES and BMS could be observed (Wallace et al., 2012; Fusaro et al., 2013). Within the DES group, no significant difference in the proliferation area was found, however there is a trend separating “limus” eluting stents (Xience: everolimus, Resolute Integrity: zotarolimus) and paclitaxel eluting stents (PES). These findings are congruent with most clinical studies describing higher ISR rates with PES (Schomig et al., 2007; Mehilli et al., 2010; Otake et al., 2010; Gao et al., 2014). Therefore, even with a very small number of tested stents this model was able to reflect the clinically well-known differences between BMS and DES and also between “limus” eluting stents and PES.

The advantage of the presented model over cell cultures lies in the direct comparison of stented vessels. The clinical effect of a DES is not only dependent on its antirestenotic drug, but also on the stent platform and the polymer carrying the drug. The interaction of these components cannot be simulated by a plain two-dimensional cell culture, which is normally used for simple cell proliferation experiments. By its three-dimensional assembly, this *in vitro* model is able to model the luminal narrowing as well as the vessel wall structure after stent implantation.

The main limitation factor of the study is the absence of blood cells and therefore the lack of their signals. *In vivo*, inflammatory cells of the blood, amongst others, mediate the migration to and proliferation of the SMCs in the neointima. To compensate this shortcoming we continued cell seeding for up to 3 months after stent implantation; however, the co-cultivation of a blood cell line is warranted for further studies. The absence of the flow dynamics of the circuit and therefore of shear stress and interaction with endogenous metabolites may impair the validity of the measurements; however, these parameters have to be disregarded for *in vitro* applications.

Another limitation regards the embedded stent sections. Because the specific synthetic resin is not suitable for immunohistochemistry, stents were removed before histochemical processing and the samples were embedded in paraffin under standard conditions. Though immunohistochemical signals could be obtained, this technique results in a partial loss of the arterial architecture. A further limitation of the study design is the degree of variability concerning the 3-dimensional vessel seeding. Due to the static culturing in cell culture dishes, it was nearly impossible to obtain vessel lumina that are evenly covered by several cell layers. Permanent rotation should overcome this problem, and the use of a bioreactor is expected to yield better results in further studies.

In conclusion, a new arterial matrix reseeded with human endothelial and smooth muscle cells was successfully developed. The present data reflect the anti-proliferative effect of commercially available DES in our model, proving its validity for long-term proliferation and migration studies in stented vessels. Our test platform cannot fully replace the animal studies prior to human clinical trials; however, it has the potential to reduce them in earlier stages of drug testing.

## References

- Akin, I., Schneider, H., Ince, H. et al. (2011). Second- and third-generation drug-eluting coronary stents: Progress and safety. *Herz* 36, 190-196. <http://dx.doi.org/10.1007/s00059-011-3458-z>
- Amiel, G. E., Komura, M., Shapira, O., et al. (2006). Engineering of blood vessels from acellular collagen matrices coated with human endothelial cells. *Tissue Eng* 12, 2355-2365. <http://dx.doi.org/10.1089/ten.2006.12.2355>
- Antonova, M. L., Antonov, P. S., Marinov, G. R. et al. (2008). Viscoelastic characteristics of *in vitro* vital and devitalized rat aorta and human arterial prostheses. *Ann Biomed Eng* 36, 947-957. <http://dx.doi.org/10.1007/s10439-008-9477-0>
- Bolland, F., Korossis, S., Wilshaw, S. P. et al. (2007). Development and characterisation of a full-thickness acellular porcine bladder matrix for tissue engineering. *Biomaterials* 28, 1061-1070. <http://dx.doi.org/10.1016/j.biomaterials.2006.10.005>
- Borschel, G. H., Huang, Y. C., Calve, S. et al. (2005). Tissue engineering of recellularized small-diameter vascular grafts. *Tissue Eng* 11, 778-786. <http://dx.doi.org/10.1089/ten.2005.11.778>
- Byrne, R. A., Joner, M. and Kastrati, A. (2009). Polymer coat-



- ings and delayed arterial healing following drug-eluting stent implantation. *Minerva Cardioangiol* 57, 567-584.
- Dahl, S. L., Koh, J., Prabhakar, V. et al. (2003). Decellularized native and engineered arterial scaffolds for transplantation. *Cell Transplant* 12, 659-666.
- Dangas, G. D., Claessen, B. E., Caixeta, A. et al. (2010). In-stent restenosis in the drug-eluting stent era. *J Am Coll Cardiol* 56, 1897-1907. <http://dx.doi.org/10.1016/j.jacc.2010.07.028>
- Fitzpatrick, J. C., Clark, P. M. and Capaldi, F. M. (2010). Effect of decellularization protocol on the mechanical behavior of porcine descending aorta. *Int J Biomater* 2010, Article ID 620503. <http://dx.doi.org/10.1155/2010/620503>
- Fusaro, M., Cassese, S., Ndrepepa, G. et al. (2013). Drug-eluting stents for revascularization of infrapopliteal arteries: Updated meta-analysis of randomized trials. *JACC Cardiovasc Interv* 6, 1284-1293. <http://dx.doi.org/10.1016/j.jcin.2013.08.007>
- Gao, L., Hu, X., Hou, Y. et al. (2014). Long time clinical outcomes of limus-eluting stent versus paclitaxel-eluting stent in patients undergoing percutaneous coronary artery intervention: A meta-analysis of randomized controlled clinical trials. *Cardiol J* 21, 211-219. <http://dx.doi.org/10.5603/CJ.a2014.0004>
- Gilbert, T. W., Sellaro, T. L. and Badylak, S. F. (2006). Decellularization of tissues and organs. *Biomaterials* 27, 3675-3683. <http://dx.doi.org/10.1016/j.biomaterials.2006.02.014>
- Gruberg, L., Waksman, R., Satler, L. F. et al. (2000). Novel approaches for the prevention of restenosis. *Expert Opin Investig Drugs* 9, 2555-2578. <http://dx.doi.org/10.1517/13543784.9.11.2555>
- Gui, L. and Niklason, L. E. (2014). Vascular tissue engineering: Building perfusable vasculature for implantation. *Curr Opin Chem Eng* 3, 68-74. <http://dx.doi.org/10.1016/j.coche.2013.11.004>
- Haase, D., Schmidl, S., Ewald, C. et al. (2010). Fatty acid synthase as a novel target for meningioma therapy. *Neuro Oncol* 12, 844-854. <http://dx.doi.org/10.1093/neuonc/noq004>
- Jo, W. M., Sohn, Y. S., Choi, Y. H. et al. (2007). Modified acellularization for successful vascular xenotransplantation. *J Korean Med Sci* 22, 262-269.
- Katz, G., Harchandani, B. and Shah, B. (2015). Drug-eluting stents: The past, present, and future. *Curr Atheroscler Rep* 17, 485. <http://dx.doi.org/10.1007/s11883-014-0485-2>
- Kimuli, M., Eardley, I. and Southgate, J. (2004). In vitro assessment of decellularized porcine dermis as a matrix for urinary tract reconstruction. *BJU Int* 94, 859-866. <http://dx.doi.org/10.1111/j.1464-410X.2004.05047.x>
- Kolh, P., Windecker, S., Alfonso, F. et al. (2014). 2014 ESC/EACTS Guidelines on myocardial revascularization: The Task Force on Myocardial Revascularization of the European Society of Cardiology (ESC) and the European Association for Cardio-Thoracic Surgery (EACTS). Developed with the special contribution of the European Association of Percutaneous Cardiovascular Interventions (EAPCI). *Eur J Cardiothorac Surg* 46, 517-592. <http://dx.doi.org/10.1093/ejcts/ezu366>
- Lloyd-Jones, D., Adams, R., Carnethon, M. et al. (2009). Heart disease and stroke statistics – 2009 update: A report from the American Heart Association Statistics Committee and Stroke Statistics Subcommittee. *Circulation* 119, 480-486. <http://dx.doi.org/10.1161/CIRCULATIONAHA.108.191259>
- McFetridge, P. S., Daniel, J. W., Bodamyali, T. et al. (2004). Preparation of porcine carotid arteries for vascular tissue engineering applications. *J Biomed Mater Res A* 70, 224-234. <http://dx.doi.org/10.1002/jbm.a.30060>
- Mehilli, J., Byrne, R. A., Tiroch, K. et al. (2010). Randomized trial of paclitaxel- versus sirolimus-eluting stents for treatment of coronary restenosis in sirolimus-eluting stents: The ISAR-DESIRE 2 (Intracoronary Stenting and Angiographic Results: Drug Eluting Stents for In-Stent Restenosis 2) study. *J Am Coll Cardiol* 55, 2710-2716. <http://dx.doi.org/10.1016/j.jacc.2010.02.009>
- Nakazawa, G., Finn, A. V., Ladich, E. et al. (2008). Drug-eluting stent safety: Findings from preclinical studies. *Expert Rev Cardiovasc Ther* 6, 1379-1391. <http://dx.doi.org/10.1586/14779072.6.10.1379>
- Nakazawa, G., Otsuka, F., Nakano, M. et al. (2011). The pathology of neoatherosclerosis in human coronary implants bare-metal and drug-eluting stents. *J Am Coll Cardiol* 57, 1314-1322. <http://dx.doi.org/10.1016/j.jacc.2011.01.011>
- Otake, H., Ako, J., Yamasaki, M. et al. (2010). Comparison of everolimus- versus paclitaxel-eluting stents implanted in patients with diabetes mellitus as evaluated by three-dimensional intravascular ultrasound analysis. *Am J Cardiol* 106, 492-497. <http://dx.doi.org/10.1016/j.amjcard.2010.03.059>
- Pfisterer, M., Brunner-La Rocca, H. P., Buser, P. T. et al. (2006). Late clinical events after clopidogrel discontinuation may limit the benefit of drug-eluting stents: An observational study of drug-eluting versus bare-metal stents. *J Am Coll Cardiol* 48, 2584-2591. <http://dx.doi.org/10.1016/j.jacc.2006.10.026>
- Rieder, E., Kasimir, M. T., Silberhumer, G. et al. (2004). Decellularization protocols of porcine heart valves differ importantly in efficiency of cell removal and susceptibility of the matrix to recellularization with human vascular cells. *J Thorac Cardiovasc Surg* 127, 399-405. <http://dx.doi.org/10.1016/j.jtcvs.2003.06.017>
- Rieder, E., Nigisch, A., Dekan, B. et al. (2006). Granulocyte-based immune response against decellularized or glutaraldehyde cross-linked vascular tissue. *Biomaterials* 27, 5634-5642. <http://dx.doi.org/10.1016/j.biomaterials.2006.06.020>
- Rosanio, S., Tocchi, M., Patterson, C. et al. (1999). Prevention of restenosis after percutaneous coronary interventions: The medical approach. *Thromb Haemost* 82, Suppl 1, 164-170.
- Roy, S., Silacci, P. and Stergiopoulos, N. (2005). Biomechanical properties of decellularized porcine common carotid arteries. *Am J Physiol Heart Circ Physiol* 289, H1567-1576. <http://dx.doi.org/10.1152/ajpheart.00564.2004>
- Salabei, J. K. and Hill, B. G. (2014). Autophagic regulation of smooth muscle cell biology. *Redox Biol* 4C, 97-103. <http://dx.doi.org/10.1016/j.redox.2014.12.007>
- Sanchez, O. D., Yahagi, K., Koppa, T. et al. (2015). The everolimus-eluting Xiencel stent in small vessel disease: Bench, clinical, and pathology view. *Med Devices (Auckl)* 8,

- 37-45. <http://dx.doi.org/10.2147/MDER.S50051>
- Schaner, P. J., Martin, N. D., Tulenko, T. N. et al. (2004). Decellularized vein as a potential scaffold for vascular tissue engineering. *J Vasc Surg* 40, 146-153. <http://dx.doi.org/10.1016/j.jvs.2004.03.033>
- Schomig, A., Dibra, A., Windecker, S. et al. (2007). A meta-analysis of 16 randomized trials of sirolimus-eluting stents versus paclitaxel-eluting stents in patients with coronary artery disease. *J Am Coll Cardiol* 50, 1373-1380. <http://dx.doi.org/10.1016/j.jacc.2007.06.047>
- Sheth, S. D. and Giugliano, R. P. (2014). Coronary artery stents: Advances in technology. *Hosp Pract (1995)* 42, 83-91. <http://dx.doi.org/10.3810/hp.2014.10.1145>
- Stefanini, G. G. and Holmes, D. R., Jr. (2013). Drug-eluting coronary-artery stents. *N Engl J Med* 368, 254-265. <http://dx.doi.org/10.1056/NEJMra1210816>
- Stettler, C., Wandel, S., Allemann, S. et al. (2007). Outcomes associated with drug-eluting and bare-metal stents: A collaborative network meta-analysis. *Lancet* 370, 937-948. [http://dx.doi.org/10.1016/S0140-6736\(07\)61444-5](http://dx.doi.org/10.1016/S0140-6736(07)61444-5)
- Teebken, O. E., Puschmann, C., Breitenbach, I. et al. (2009). Preclinical development of tissue-engineered vein valves and venous substitutes using re-endothelialised human vein matrix. *Eur J Vasc Endovasc Surg* 37, 92-102. <http://dx.doi.org/10.1016/j.ejvs.2008.10.012>
- Wallace, E. L., Abdel-Latif, A., Charnigo, R. et al. (2012). Meta-analysis of long-term outcomes for drug-eluting stents versus bare-metal stents in primary percutaneous coronary interventions for ST-segment elevation myocardial infarction. *Am J Cardiol* 109, 932-940. <http://dx.doi.org/10.1016/j.amjcard.2011.11.021>
- Williams, C., Liao, J., Joyce, E. M. et al. (2009). Altered structural and mechanical properties in decellularized rabbit carotid arteries. *Acta Biomater* 5, 993-1005. <http://dx.doi.org/10.1016/j.actbio.2008.11.028>

#### Conflict of interest

The authors declare that no conflict of interest exists.

#### Acknowledgments

The work was supported by grant 031A225 from the German Bundesministerium für Bildung und Forschung (BMBF) and by local institutional funding. We are grateful to Ms. Johanna Gunkel and Mr. Carlheinz Holzfuß from the University of Applied Sciences in Jena for kind assistance with the stretch test. We thank Ms. Ines Thiele from the Chair of Materials Science in Jena for technical help with the embedding of stented samples.

#### Correspondence to

Daniela Haase, PhD  
University Hospital Jena  
Clinic of Internal Medicine I  
Erlanger Allee 101  
07743 Jena, Germany  
Phone: +49 3641 9324758 / +49 3641 9324113  
Fax: +49 3641 9324102  
e-mail: daniela.haase@med.uni-jena.de

## Erratum

# Erratum to Regulatory Acceptance and Use of Serology for Inactivated Veterinary Rabies Vaccines

Marie-Jeanne W. A. Schiffelers<sup>1</sup>, Bas J. Blaauboer<sup>2</sup>, Wieger E. Bakker<sup>1</sup> and Coenraad F. M. Hendriksen<sup>3</sup>

<sup>1</sup>Utrecht University School of Governance, Utrecht, The Netherlands; <sup>2</sup>Utrecht University, Institute for Risk Assessment Sciences (IRAS), Utrecht, The Netherlands; <sup>3</sup>Institute for Translational Vaccinology (Intravacc), Bilthoven & Utrecht University, Faculty of Veterinary Medicine, Department Animals in Science and Society, The Netherlands

This manuscript which appeared in ALTEX (2015), 32(3), 211-221, <http://dx.doi.org/10.14573/altex.1501261> should have been designated a Research Article and not a Review Article.